Micro- and nanoelectronics. Condensed matter physics

Микро- и наноэлектроника. Физика конденсированного состояния

UDC 538.955
https://doi.org/10.32362/2500-316X-2025-13-4-37-46
EDN WYJGOZ

RESEARCH ARTICLE

Measurement of magnetostriction using a strain gauge bridge with alternating excitation

Dmitry A. Burdin @

MIREA – Russian Technological University, Moscow, 119454 Russia
@ *Corresponding author, e-mail: phantastic@mail.ru*

• **Submitted:** 21.11.2024 • **Revised:** 15.01.2025 • **Accepted:** 20.05.2025

Abstract

Objectives. Knowledge of the dependence of magnetostriction of various ferromagnetic materials on the magnetic field is important for studying the magnetoelectric effect in composite structures, in particular for calculating the shape of the field dependence of piezomagnetic moduli and for calculating magnetoelastic characteristics. However, the typical resolution level of known strain gauge setups for measuring magnetostriction is about 10^{-6}, which is insufficient to obtain detailed information on the piezomagnetic coefficients of the materials under study. The paper describes the development of an automated setup for the precision measurement of the dependence of magnetostriction of ferromagnetic plates on a magnetic field in the range of ±5 kOe providing an improved strain resolution order of magnitude.

Methods. The setup uses film strain gauges included in a Wheatstone bridge excited by alternating current. Thanks to the applied method of signal frequency shift, as well as the use of a low-noise preamplifier and temperature stabilization of the measuring cell, it was possible to reduce the level of noise referred to the input and zero drift of the measuring circuit.

Results. The developed setup provides an accuracy of the magnetostriction measurement of ferromagnetic plates up to 10^{-7} in the range of magnetic fields of ±5 kOe, which is an order of magnitude higher than known methods. The setup also allows measuring the electric and piezoelectric deformation of materials depending on the applied electrical voltage in the range of ±500 V. The measurement results can be used to more accurately calculate the field dependencies of the piezomagnetic and piezoelectric coefficients of materials, including materials with low magnetostriction, such as various ferrites, hematite, yttrium iron garnet, etc.

Conclusions. The method of alternating excitation of the measuring bridge in combination with other measures can be used to increase the deformation resolution to about 10^{-7}.

Keywords: magnetostriction, strain gauge, deformation, magnetoelectric effect, composite structure

For citation: Burdin D.A. Measurement of magnetostriction using a strain gauge bridge with alternating excitation. *Russian Technological Journal.* 2025;13(4):37–46. https://doi.org/10.32362/2500-316X-2025-13-4-37-46, https://www.elibrary.ru/WYJGOZ

Financial disclosure: The author has no financial or proprietary interest in any material or method mentioned.

The author declares no conflicts of interest.

НАУЧНАЯ СТАТЬЯ

Измерение магнитострикции тензометрическим мостом с переменным возбуждением

Д.А. Бурдин @

МИРЭА – Российский технологический университет, Москва, 119454 Россия
@ *Автор для переписки, e-mail: phantastic@mail.ru*

• **Поступила:** 21.11.2024 • **Доработана:** 15.01.2025 • **Принята к опубликованию:** 20.05.2025

Резюме

Цели. Знание зависимости магнитострикции различных ферромагнитных материалов от магнитного поля важно для исследования магнитоэлектрического эффекта в композитных структурах, в частности для расчета формы полевой зависимости пьезомагнитных модулей и расчета магнитоупругих характеристик. Наиболее распространенным методом измерения магнитострикционного удлинения является использование тензорезистивных датчиков. Однако типичный уровень разрешения известных тензорезистивных установок для измерения магнитострикции составляет около 10^{-6}, что недостаточно для получения детальной информации о пьезомагнитных коэффициентах исследуемых материалов. Цель работы – разработка автоматизированной установки для прецизионного измерения зависимости магнитострикции ферромагнитных пластин от магнитного поля в диапазоне ±5 кЭ с улучшенным на порядок разрешением по деформации.

Методы. В установке использованы пленочные тензорезистивные датчики, включенные в мост Уитстона, возбуждаемый переменным током. Благодаря примененному методу переноса частоты сигнала, а также применению малошумящего предусилителя и температурной стабилизации измерительной ячейки, удалось уменьшить уровень приведенных ко входу шумов и дрейфа нуля измерительной схемы.

Результаты. Созданная установка обеспечивает на порядок более высокую точность измерения магнитострикции ферромагнитных пластин, чем известные, до 10^{-7} в диапазоне магнитных полей ±5 кЭ. Установка позволяет измерять также электро- и пьезодеформацию материалов в зависимости от приложенного электрического напряжения в диапазоне ±500 В. Результаты измерений дают возможность более точно рассчитать полевые зависимости пьезомагнитных и пьезоэлектрических коэффициентов материалов, в т.ч. материалов с малой величиной магнитострикции, таких как различные ферриты, гематит, железо-иттриевый гранат и др.

Выводы. Применение метода переменного возбуждения измерительного моста в совокупности с другими мерами позволило повысить разрешение по деформации, которое составило около 10^{-7}.

Ключевые слова: магнитострикция, тензометр, деформация, магнитоэлектрический эффект, композитная структура

Для цитирования: Бурдин Д.А. Измерение магнитострикции тензометрическим мостом с переменным возбуждением. *Russian Technological Journal*. 2025;13(4):37–46. https://doi.org/10.32362/2500-316X-2025-13-4-37-46, https://www.elibrary.ru/WYJGOZ

Прозрачность финансовой деятельности: Автор не имеет финансовой заинтересованности в представленных материалах или методах.

Автор заявляет об отсутствии конфликта интересов.

INTRODUCTION

Magnetostriction describes the change in the linear dimensions of a ferromagnet when its magnetization is changed. One of the main features of magnetostriction is the saturation magnetostriction λ_{sat}, which is equal to the relative elongation of the sample in the magnetic saturation field H_s. However, the dependence of the relative elongation on the magnetic field $\lambda(H)$ provides a more thorough description of the magnetostriction properties. The ability to measure the dependence of magnetostriction of different ferromagnetic materials on the magnetic field is important for studies of magnetoelectric (ME) effects in composite structures containing ferromagnetic (FM) and piezoelectric (PE) layers, as well as for the development of new smart devices [1–3]. ME effects in such structures arise from the interaction of mechanically bound FM and PE layers under the influence of external electric and magnetic fields.

Typical ME structures and their constituent layers are plates with in-plane dimensions of ~5 × 20 mm and thicknesses of tens and hundreds of micrometers. Ni ($\lambda_{sat} = -30 \cdot 10^{-6}$), Terfenol-D ($\lambda_{sat} = 2000 \cdot 10^{-6}$), amorphous alloys FeBSiC ($\lambda_{sat} = 20–30 \cdot 10^{-6}$), FeCoV ($\lambda_{sat} = 70 \cdot 10^{-6}$), and galfenol ($\lambda_{sat} = 30–90 \cdot 10^{-6}$) are used as materials for FM layers. Recently, the possibility of creating ME structures with single crystal layers of ferro- and antiferromagnetic materials with lower magnetostriction ($\lambda_{sat} < 10^{-5}$) has attracted the interest of researchers. The main methods for direct measurement of magnetostriction are strain gauges [4–8] and dilatometers [9]. Dilatometers are divided into capacitive [10, 11] and optical [12–14] according to the principle of operation. The most convenient method for studying the magnetostriction of planar FM samples and composite structures is the strain gauge method, where a strain gauge resistor is bonded to the sample and included in the measuring bridge. This method is widely used for magnetostriction measurements due to its low cost and the ease of sample preparation. However, disadvantages include its limited applicability for measuring the magnetostriction of films.

In such systems, the measuring bridge is typically powered by a constant voltage (current) source, which imposes restrictions on the minimum resolvable strain magnitude. Such strain gauges have a typical input noise spread of $(2–5) \cdot 10^{-6}$ [15–17], which is acceptable for the study of materials with large saturation magnetostriction $\lambda_{sat} > 10^{-5}$, but cannot be used to study materials having low magnetostriction. In order to solve this problem, it will be necessary to create a setup offering a higher resolution.

The aim of this work is to develop a setup for measuring magnetostriction by the strain gauge method with a higher resolution (better than 10^{-6}). The first part of the paper describes the design of the setup, followed by a description of the operating principle and an analysis of the noise determining the resolution. The final part of the paper deals with the practical verification of the achieved level of input noise and the demonstration of magnetostriction and electrostriction measurements on real samples.

SETUP DESIGN

The external view of the proposed magnetostriction measurement setup is shown in Fig. 1. It consists of three main parts (Fig. 2): magnetic system, measuring cell, and control and measuring unit (CMU). The magnetic system used to generate a constant magnetic field of 0 to 5 kOe represents a laboratory electromagnet with a measuring cell on a movable base and a probe with a Hall sensor installed in the magnetic gap. The movable base of the cell is used for positioning the cell in the gap of the electromagnet and operative removal of the sample (board with the sample). The cell is moved by means of a carriage moving on a rail guide installed between the poles of the electromagnet.

In order to power the electromagnet, a standard laboratory power supply fitted with a switching device for switching the magnetic field polarity is used. The magnetic field is measured using a Lake Shore 421 laboratory gaussmeter (Lake Shore, USA).

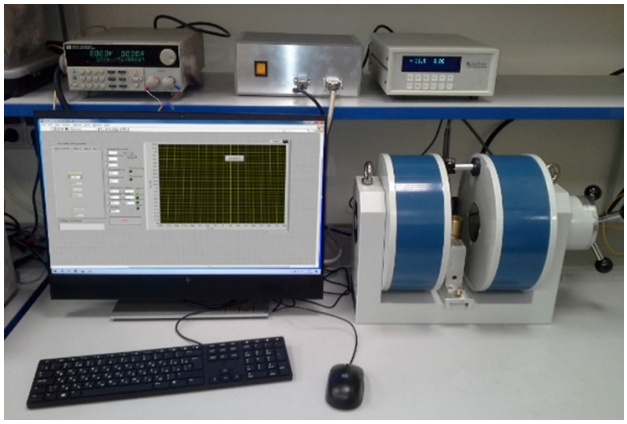

Fig. 1. External view of the magnetostriction measurement setup

The sample to be tested is placed on the removable board of the measuring cell with a strain gauge glued to its surface. The leads of the strain gauge are soldered to the contact pads to form a Wheatstone bridge together with the resistors on this board. Balancing circuits (based on a wire potentiometer) and a preamplifier are implemented on the same board.

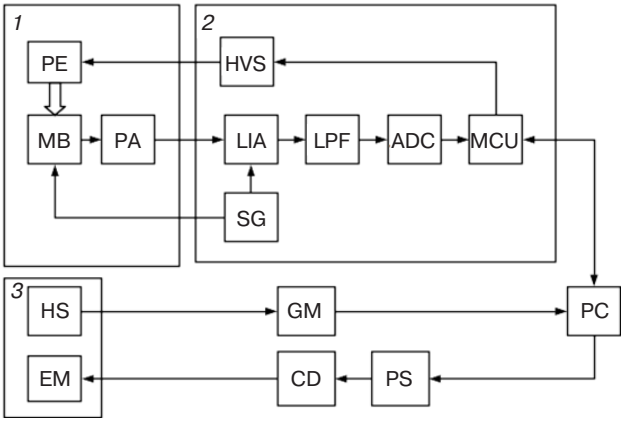

Fig. 2. Schematic diagram of the magnetostriction measurement setup: *1* is a measuring cell, *2* is a CMU, and *3* is a magnetic system; PE is a PE element, MB is a measuring bridge, PA is a preamplifier, LIA is a lock-in amplifier, HVS is a high voltage power supply, SG is a signal generator, LPF is a low pass filter, ADC is an analogue-to-digital converter, MCU is a microcontroller unit, HS is a Hall sensor, EM is an electromagnet, GM is a gaussmeter, CD is a commutation device, PS is a power supply for an electromagnet, and PC is a personal computer

The cell on the base (the electromagnet is shown in cross-section) is shown in Fig. 3. The cell body, which has a cylindrical shape, can be rotated 180° around the vertical axis using a removable handle, allowing orientation-dependent measurements. The angle of the cell orientation is measured on a scale on the side (cylindrical) surface of its body.

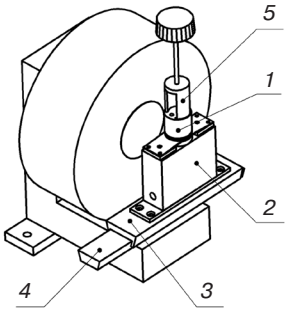

Fig. 3. Cell on the base (construction and external view): (*1*) cell, (*2*) base radiator, (*3*) cell carriage, (*4*) base rail, and (*5*) removable handle

The removable amplifier board is as shown in Fig. 4a. The board with the sample is mounted on top of the Peltier module and connected to the base board by two small six pin connectors. A thermoelectric component is used to stabilize the temperature of the sample plate with an accuracy of 0.01°C. The electrical cable connecting the cell to the CMU is connected to the base board and the thermoelectric cell via pins on the underside of the cell body. The preamplifier is based on a low noise integrated instrument amplifier INA849 (Texas Instruments, USA).

The CMU is used to acquire and digitize the measuring signal, to stabilize the temperature of the sample plate, to supply the bridge with alternating voltage at a frequency of 410 Hz and an amplitude of up to 4 V, and to generate a constant voltage from −500 to 500 V for the study of electrostriction and PE samples. The CMU is housed in a table-top case with dimensions of 300 × 150 × 100 mm. The CMU and the cell are connected by a 15-pin signal cable.

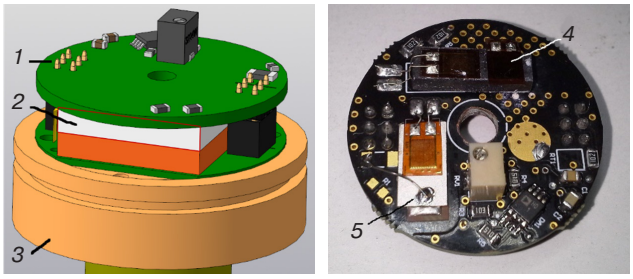

(a) (b)

Fig. 4. Cell design (a) and external view of removable amplifier board (b): (*1*) amplifier board; (*2*) Peltier module; (*3*) cell base; (*4*) FM sample with strain gauge; (*5*) piezoelectric element with strain gauge

STRAIN GAUGE OPERATING PRINCIPLE

The elongation of the sample is measured using standard strain gauges. A foil strain gauge is a meandering grid of thin metal foil on a paper or polyimide substrate. The sensor is bonded to the sample surface taking into account the direction of sensitivity. The two basic sensor configurations are shown in Fig. 5.

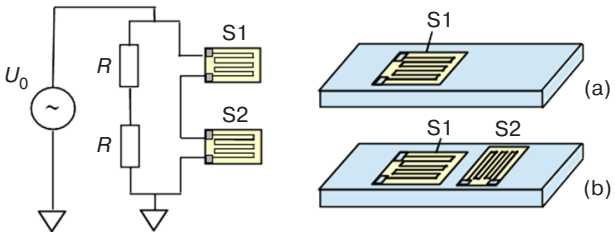

Fig. 5. Strain gauge half-bridge: (a) with one active sensor; (b) with two active sensors

Here, one arm of the bridge is made up of two resistors of the same resistance *R* and the other arm is made up of two strain gauges S1 and S2. In the first case, only one sensor (S1) is bonded to the sample, while the second sensor (S2) only complements the arm of the measuring bridge. This configuration is used when it is necessary to selectively measure elongation in one direction. If the deformation is along the side

of the sample, the second configuration can be used, in which the reference sensor S2 is bonded to the sample (on the same or opposite surface) at an angle of 90° to the first.

Figure 6 depicts the functional diagram of the analogue part of the strain gauge signal path, consisting of the preamplifier K_{amp}, the demodulator on the AD630 chip (Analog Devices, Inc., USA), and the low-pass filter. We consider the conversion of the signal from the measuring bridge to the ADC input. The bridge is fed by the harmonic voltage u_b with amplitude U_0 and frequency ω_0: $u_b = U_0\cos(\omega_0 t)$, where t is time. It can be shown that the unbalanced voltage of the bridge under signal modulated $u_{s.m.} \approx u_b \delta R/4$, where δR is the change in resistance of the strain gauge.

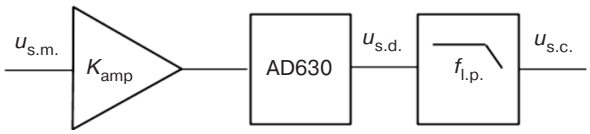

Fig. 6. Analogue part of the input measurement path: $u_{s.m.}$ is the bridge imbalance voltage; $u_{s.d.}$ is the signal at the demodulator output; $f_{l.p.}$ is the low pass filter cut-off frequency; $u_{s.c.}$ is the signal at the ADC input

Let the periodic deformation $\varepsilon = \varepsilon_0\cos(\omega t)$ occur at the frequency $\omega < \omega_0$, with $\delta R = G\varepsilon_0\cos(\omega t)$, where ε_0 is the strain amplitude, and $G \approx 2$ is the strain sensitivity coefficient of the sensor. Then the bridge imbalance voltage is as follows:

$$u_{s.m.} \approx \frac{u_b \delta R}{4} = \frac{U_0\cos(\omega_0 t) G\varepsilon_0 \cos(\omega t)}{4} = \\ = \frac{\frac{1}{2}U_0 G\varepsilon_0 (\cos((\omega_0 - \omega)t) + \cos((\omega_0 + \omega)t))}{4}. \quad (1)$$

Thus, the useful signal, which is proportional to the change in resistance of the strain gauge on the sample, modulates the voltage amplitude. As a result, the signal spectrum is shifted to the frequencies $(\omega_0 + \omega)$ and $(\omega_0 - \omega)$ at the right and left sidebands. In the case of constant strain ($\omega \approx 0$), equation (1) is simplified as follows:

$$u_{s.m.} \approx \frac{u_b \delta R}{4} = \frac{U_0\cos(\omega_0 t) G\varepsilon_0}{4}. \quad (2)$$

The signal $u_{s.m.}$ is amplified by the preamplifier with a gain $K_{amp} \approx 1000$ and is fed to the input of a lock-in amplifier, which is realized with AD630 chip. The signal at the output of lock-in amplifier is as follows:

$$u_{s.d.}(\omega) = K_{amp} u_{s.m.}(\omega)\cos(\omega_0 t) = \\ = \frac{K_{amp} U_0 \cos(\omega t) G\varepsilon_0 \cos^2(\omega_0 t)}{4} = \\ = \left[\frac{K_{amp} U_0 G\varepsilon_0}{8}(1 + 2\cos(\omega_0 t))\right]_{\omega=0}. \quad (3)$$

This means that the original signal is restored and there is an additional component with a frequency of $2\omega_0$. The third-order low-pass filter (LPF), which is located after the detector and has a bandwidth of $\omega_{l.p.} << \omega_0$ ($\omega_{l.p.} \approx 14$ Hz), cuts off the high-frequency components of the signal before the analogue-to-digital conversion. The filter has the following transfer characteristic:

$$K_{l.p.} = \frac{1}{\left(\sqrt{1 + \left(\frac{\omega}{\omega_{l.p.}}\right)}\right)^3}. \quad (4)$$

As a result, the signal at the ADC input is as follows:

$$u_{s.c.}(\omega) = \frac{K_{amp} K_{l.p.} U_0 G\varepsilon_0 \cos(\omega t)}{8} = \\ = \left[\frac{K_{amp} K_{l.p.} U_0 G\varepsilon_0}{8}\right]_{\omega=0}. \quad (5)$$

Following digitization, the signal is smoothed using the simple moving average algorithm. The window size is set within 1–250 samples, and the sample frequency is 250 s^{-1}.

STRAIN GAUGE AMPLIFIER NOISE ANALYSIS

In the analysis of the electrical noise in the strain gauge circuit, only the input noise is considered, since the preamplifier has a high gain (about 1000) and the influence of the noise in the subsequent stages is negligible. The possible sources of this noise are considered.

Thermal noise. Thermal noise (Nyquist noise) is caused by thermal oscillations of charge carriers in conductors, and it is generated constantly, regardless of the current flowing. The spectrum of thermal noise is broadband and uniform, and the power spectral density of a resistor with resistance R is given by the following expression [18]:

$$S_n = 4kTR, \quad (6)$$

where S_n is the spectral voltage density of the thermal noise $\left(V/\sqrt{Hz}\right)$, k = 1.38 · 10^{-23} J/K is

the Boltzmann constant, and T is the absolute temperature. The thermal noise is characteristic of all resistors and is marked as the source of S_n in the diagram (Fig. 7).

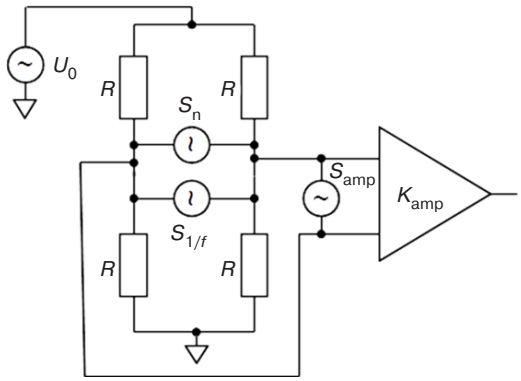

Fig. 7. Main sources of noise in the input circuits. S_{amp} is the amplifier noise

Flicker noise (1/*f*). Flicker noise is characterized by a specific frequency dependence of the spectral density, generally described by the following equation [19]:

$$S_{1/f} = \sqrt{\frac{CR^{\beta}I^{\beta}}{f^{\gamma}}}, \tag{7}$$

where $S_{1/f}$ is the spectral density of the flicker noise voltage $\left(\mathrm{V}/\sqrt{\mathrm{Hz}}\right)$, while C, β and γ are coefficients, I is the intensity of the current flowing, and f is the frequency. For metallic films at relatively low values of current density, β = 2 and γ = 1 can be accepted. The flicker noise of the conductor is assumed to be equivalent to the change in its resistance due to fluctuations in the mobility of the charge carriers during scattering on the lattice or fluctuations in the equilibrium temperature [20]. The flicker noise is denoted by the source $S_{1/f}$ in Fig. 7.

Amplifier noise. Amplifier noise is the combined noise of all sources in an instrument amplifier, represented as an equivalent noise voltage source at the amplifier input (S_{amp} in Fig. 7). Since the current noise density for this chip is approximately $1.1\,\mathrm{pA}/\sqrt{\mathrm{Hz}}$, it can be neglected given the low impedance of the input circuits.

The sources of electrical noise in the circuit in Fig. 7 can therefore be divided into 2 types: additive and multiplicative. Additive noise is voltage and current noise; as such, it does not modulate the pump signal and its spectrum does not change. Multiplicative noise, which comprises fluctuations in the resistances of the bridge resistors, causes a change in the balance of the bridge; as a result of amplitude modulation (AM), its spectral density function is transformed in the same way as a useful signal. Let S_{in} be the spectral density of the noise voltage at the amplifier input at a constant bridge supply voltage; when the bridge is supplied with an alternating voltage of frequency ω, it is transformed into modulated $S_{in.mod.}$:

$$\begin{gathered} S_{in}^2 = S_n^2(\omega) + S_{amp}^2(\omega) + \\ + S_{1/f}^2(\omega) \overset{AM}{\rightarrow} S_{in.mod.}^2(\omega) = \\ = S_n^2(\omega) + S_{amp}^2(\omega) + \frac{1}{4}S_{1/f}^2(\omega_0 - \omega) + \\ + \frac{1}{4}S_{1/f}^2(\omega_0 + \omega). \end{gathered} \tag{8}$$

The fact that for a balanced bridge the output noise is equivalent to the noise of one of the resistors is used here. It can be shown that the spectral density of the noise at the demodulator output S_d is described by the following expression:

$$\begin{gathered} S_d^2(\omega) = K_{amp}^2 \times \\ \times \left(\frac{1}{2}S_n^2(\omega + \omega_0) + \frac{1}{2}S_{amp}^2(\omega + \omega_0) + \frac{1}{4}S_{1/f}^2(\omega) \right). \end{gathered} \tag{9}$$

The spectral density $S_{in.conv.}$ of the noise at the ADC input is as follows:

$$\begin{gathered} S_{in.conv.}^2(\omega) = K_{amp}^2 K_{l.p.}^2 \times \\ \times \left(\frac{1}{2}S_n^2(\omega + \omega_0) + \frac{1}{2}S_{amp}^2(\omega + \omega_0) + \frac{1}{4}S_{1/f}^2(\omega) \right). \end{gathered} \tag{10}$$

The resolution of the strain gauge can be estimated by the total noise level. The value of the noise voltage u_Σ referred to the input (RTI) is obtained by integrating equation (10) and dividing by the gain, as follows:

$$u_\Sigma = \frac{\int_{\omega_l}^{\omega_h} S_{in.conv.}^2(\omega)d\omega}{K_{amp}} = \sqrt{\int_{\omega_l}^{\omega_h} \left(K_{l.p.}^2 \frac{1}{4}S_{1/f}^2(\omega) + K_{l.p.}^2 \frac{1}{2}S_n^2(\omega + \omega_0) + K_{l.p.}^2 \frac{1}{2}S_{amp}^2(\omega + \omega_0) \right) d\omega}. \tag{11}$$

The flicker-noise voltage spectral density $S_{1/f}$ of the 1-XY33-6 standard constantan strain gauges measured in [21] is used in the calculations. Substituting the data into expression (11) and taking into account (6) and (7), the level of the mean square noise voltage referred to the input is $u_\Sigma = 6.7 \cdot 10^{-9}$ V. Knowing the input noise level and taking into account expression (1), the mean square value of the apparent elongation can be expressed as follows:

$$\sigma_\varepsilon = \frac{4u_\Sigma}{u_b G} = \frac{4 \cdot 1.1 \cdot 10^{-8}}{1.5 \cdot 2} = \\ = 1.46 \cdot 10^{-8} = 0.015 \cdot 10^{-6}. \quad (12)$$

The following equation can be used to estimate the noise amplitude value (noise trace width) $\Delta\varepsilon_{pp}$ (peak-to-peak):

$$\Delta\varepsilon_{pp} \approx 6\sigma_\varepsilon = 0.888 \cdot 10^{-6}. \quad (13)$$

By the described means, the limits of the electrical noise on the resolution of the strain gauge are determined. According to calculations, the main contribution to the electrical noise level is made by the flicker noise of the measuring bridge resistor. However, in addition to the electrical noise, there are a number of other factors that affect the elongation measurement result.

Selecting the modulation frequency. From the above analysis, it is clear that the modulation frequency of the strain bridge should be selected to provide sufficient detuning from the low frequency portion of the noise spectrum of the instrument amplifier. On the other hand, increasing the modulation frequency will increase the influence of parasitic reactive elements. Detuning from the industrial frequency (50 Hz) and its harmonics is also required. Taking these factors into account, a frequency of 410 Hz is selected.

Temperature fluctuations and drift. The temperature of the bridge elements can only be regarded as approximately uniform and constant. In reality, there are temperature fluctuations and drifts due to the processes of power dissipation generated by the strain gauges and the instrument amplifier, as well as the instability of the laboratory temperature.

A typical value for the temperature resistance coefficient (TRC) of a constantan strain gauge is TRC = $10 \cdot 10^{-6}$ 1/K. The temperature change causing the false response to the noise trace width is estimated as follows:

$$\Delta T = \frac{\Delta\varepsilon_{pp}}{TRC} = 0.009 \text{ K}. \quad (14)$$

It can be seen that the strain gauge circuit is extremely sensitive to nonuniform temperature changes. However, equation (14) does not take into account the effect of the difference between the thermal expansion coefficients (TEC) of the sample plate and the gauge [15] $\Delta TEC = TEC_{sam.pl.} - TEC_{gauge}$, which can increase the thermal sensitivity several times:

$$\Delta T = \frac{\Delta\varepsilon_{pp}}{TRC \pm \Delta TEC \cdot G}. \quad (15)$$

In standard strain gauge applications, the temperature compensation technique is often used, in which the TRC of the strain gauges is matched to the TEC of the material, so that the sum in the denominator of expression (15) tends to zero. Unfortunately, in the case of a universal strain gauge, this method is practically inapplicable due to the sample material may be different and TEC is generally unknown. In addition, the situation is complicated by the uncertainty in the value of the thermal conductivity and thermal mass of the sample, which affects the process of heat dissipation generated by the strain gauge. The following methods were used in the design of the measurement cell to overcome the parasitic influence of thermal processes. Firstly, the cell is designed to be closed to eliminate the influence of convective air currents. After mounting the sample and balancing the bridge, a period of time is required for the temperature inside the cell to equalize. Secondly, there is active precision temperature stabilization of the amplifier board using a Peltier module. The design of the cell also allows for the balanced configuration of the active arm strain gauges of the bridge, where both resistors are bonded to the sample, thus compensating to some extent for the temperature sensitivity.

MEASUREMENT RESULTS

In order to evaluate the strain resolution of the setup, the time dependence of the strain gauge output signal in the absence of a magnetic field, $H = 0$, is recorded. The sample contains 1000 points and the recording time is 10 min. The resulting noise trace is shown in Fig. 8. The value of the standard deviation in the plot is $\sigma_\varepsilon \approx 0.016 \cdot 10^{-6}$, which corresponds to the amplitude value of the noise, $\Delta\varepsilon_{pp} = 0.096 \cdot 10^{-6}$. This result is in good agreement with the calculation according to (13).

To demonstrate the advantages of the created setup, magnetostriction curves of a magnesium ferrite sample $MgFe_2O_4$ are measured on an alternating

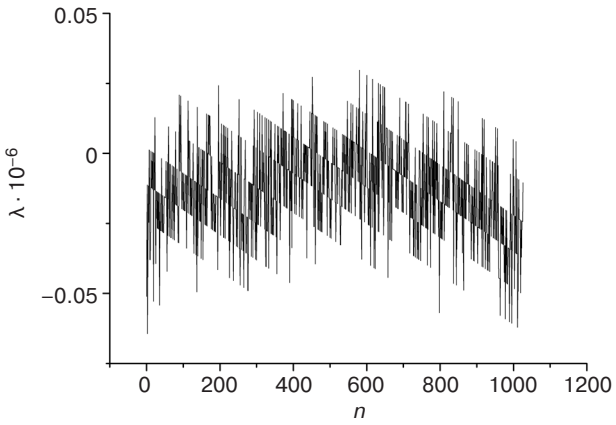

Fig. 8. Noise trace of the strain gauge setup (here, *n* is the sample number)

excitation strain gauge and on a DC strain gauge [18]. The sample is remagnetized by a limit cycle with a magnetic field step of 0.3 Oe. The difference in the noise level of the two setups is as depicted in Fig. 9. Curve *1* is much cleaner and shows the hysteresis during the remagnetization, while curve *2* only gives a qualitative view of the field dependence of the sample magnetostriction.

In order to calculate the field characteristics of ME effects, it is important to know the dependencies of the piezomagnetic coefficient $q = d\lambda/dH$ on the magnetic field. The dependencies $q(H)$ as calculated by numerical differentiation of the $\lambda(H)$ curves (Fig. 9) are shown in Fig. 10. Curve *1* is obtained using data from a strain gauge with alternating excitation, while curve *2* is obtained using data from a conventional DC strain gauge. From the curves, it can be seen that the use of an alternating excitation of the Wheatstone bridge for magnetostriction measurements allows for a much more accurate prediction of the shape of the field dependence of the linear ME effect.

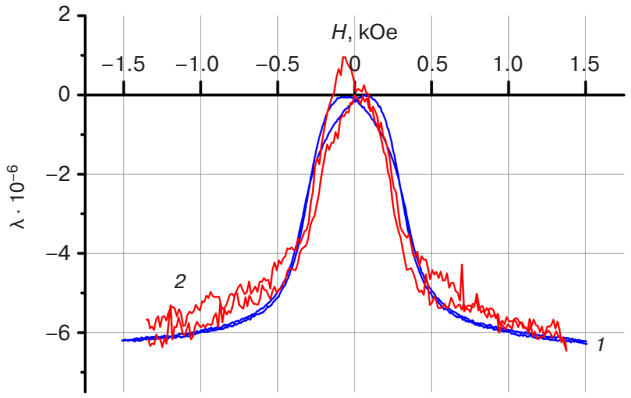

Fig. 9. Dependence of the magnetostriction λ of the $MgFe_2O_4$ plate on the magnetic field strength *H* measured by strain gauge with alternating current (AC) excitation (*1*) and strain gauge with direct current (DC) (*2*)

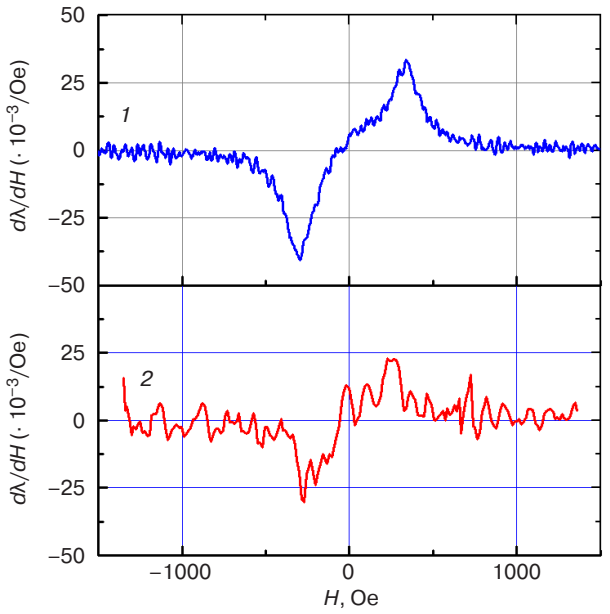

Fig. 10. Calculated dependence of the piezomagnetic coefficient *q* on the magnetic field strength *H* for the $MgFe_2O_4$ sample according to the strain gauge data: (*1*) AC, (*2*) DC

Due to the presence of a controlled bipolar high voltage source (HVS in Fig. 2), the described setup also allows the measurement of the PE effect and the investigation of electro- and magneto-acoustic interactions in composite structures. A constant voltage *U* of up to 500 V is applied to the electrodes of the PE sample to measure the deformation of the sample. The typically measured dependence of the elongation of the 5 × 10 × 0.2 mm thick polarized PZT-5 plate (Research Institute "Elpa," Russia) on the electrical voltage applied to the electrodes on its surface is shown in Fig. 11. The value of the piezoelectric module d_{31} calculated from the data in Fig. 11 at the point of zero displacement is approximately 130 pC/N, which is close to the manufacturer's specification (d_{31} = 155 pC/N).

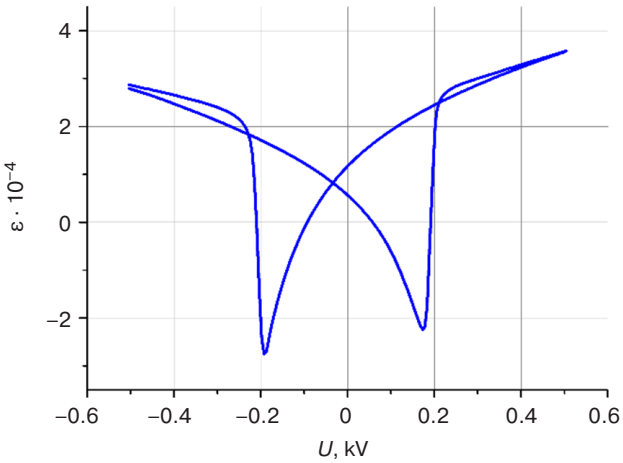

Fig. 11. Measured dependence of the PE deformation ε of the PZT-5 plate on the electrical voltage *U*

The table shows the main characteristics of the created setup (with AC excitation) in comparison to a strain gauge on a DC bridge [18]. With respect to the value of the noise referred to the input, it can be seen that the AC setup significantly outperforms the DC setup, as well as the standard strain gauge amplifier DPM911B[1] (Kyowa Electronic Instruments Co., Japan) used in [6] (RTI = 2).

Table. The setup main properties

Parameter	AC	DC [16]
Measured elongation range, μm/m	0–2000	0–2000
Noise referred to the input, μm/m	0.096	2
Maximum sample dimensions, mm × mm	20 × 10	20 × 10
Maximum magnetic field, G	5000	1500

CONCLUSIONS

The setup is developed for measuring the dependence of the magnetostrictive elongation of plate-shaped samples on the magnetic field and that of the electrostrictive/piezoelectric elongation on the electric field. It is shown that the AC excitation of the Wheatstone bridge, the use of synchronous detection, and the thermostabilization of the sample and the components of the measuring circuit allow the noise level to be reduced by almost an order of magnitude in comparison with conventional devices using DC excited Wheatstone bridge. The strain resolution of the setup is ~10^{-7}. It is determined that the main source of noise in the measurement circuit is the $1/f$ noise of the strain gauges, which, due to its nature, is indistinguishable from the useful signal in terms of signal processing methods. The measured noise level is in agreement with the calculated noise level based on published noise characteristics of film strain gauges. A further improvement of the resolution of the measurement setup can be achieved by improving the ratio between the strain sensitivity coefficient and the flicker noise level of the strain gauges.

ACKNOWLEDGMENTS

The study is supported by the Ministry of Science and Higher Education of the Russian Federation within a State Assignment for Universities (project No. FSFZ-2023-0005).

The calculation data can be provided upon request.

REFERENCES

1. Chu Z., Pourhosseini Asl M., Dong S. Review of multi-layered magnetoelectric composite materials and devices applications. *J. Phys. D: App. Phys.* 2018;51(24):243001. https://doi.org/10.1088/1361-6463/aac29b
2. Serov V.N., Fetisov L.Y., Fetisov Y.K., Shestakov E.I. High-sensitivity magnetometer based on a magnetoelectric sensor. *Rossiiskii tekhnologicheskii zhurnal.* 2016;4(5):24–37 (in Russ.). https://doi.org/10.32362/2500-316X-2016-4-5-24-37
3. Fedulov F.A., Saveliev D.V., Chashin D.V., Shishkin V.I., Fetisov Yu.K. Magnetoelectric effects in stripe- and periodic heterostructures based on nickel–lead zirconate titanate bilayers. *Russian Technological Journal*. 2022;10(3):64–73. https://doi.org/10.32362/2500-316X-2022-10-3-64-73
4. Kuczynski K., Bienkowski A., Szewczyk R. New Measuring System for Testing of the Magnetostrictive Properties of the Soft Magnetic Materials. In: *10th IMIKO TC4 Int. Workshop on ADC Modeling and testing* – IWADC. 2005. P. 434–439. Available from URL: https://www.imeko.info/publications/tc4-2005/IMEKO-TC4-2005-078.pdf
5. Linhares C.C., Santo J.E., Teixeira R.R., Coutinho C.P., Tavares S.M.O., Pinto M., Costa J.S., Mendes H., Monteiro C.S., Rodrigues A.V., Frazao O. Magnetostriction Assessment with strain gauges and fiber bragg gratings. *EAI Endorsed Trans. on Energy Web*. 2020;7(25):e4. https://doi.org/10.4108/eai.13-7-2018.161420
6. Wang Z., Fan Z., Li X., Xu K., Yu R. Measurement of magnetic and magnetostrictive characteristics of transformer core based on triaxial strain gauge and B-H vector sensor. *Sensors.* 2023;23(13):5926. http://doi.org/10.3390/s23135926
7. Pszcaola J., Cetnar T. Measurements of huge magnetostriction of the heavy rare earth – iron intermetallics. *Physics for Economy*. 2021;4:65–74.
8. Wang W., Liu H., Huang R., Zhao Y., Huang C., Guo S., Shan Y., Li L. Thermal expansion and magnetostriction measurements using the Strain Gauge Method. *Front. Chem.* 2018;6:72. https://doi.org/10.3389/fchem.2018.00072
9. Iwakami O., Kawata N., Takeshita M., Yao Y., Abe S., Matsumoto K. Thermal expansion and magnetostriction measurements using a Quantum Design Physical Property Measurement System. *J. Phys.: Conf. Ser*. 2014;568(3):032002. https://doi.org/10.1088/1742-6596/568/3/032002

[1] DPM-911B strain guage amplifer datasheet. https://product.kyowa-ei.com/en/products/amplifiers/type-s_dpm-900_series?tab=specification. Accessed May 19, 2025.

10. Kundys B., Bukhantsev Y., Vasiliev S., Kundys D., Berkowski M., Dyakonov V.P. Three terminal capacitance technique for magnetostriction and thermal expansion measurements. *Rev. Sci. Instrum.* 2004;75(6):2192–2196. https://doi.org/10.1063/1.1753088
11. Miyake A., Mitamura H., Kawachi S., Kimura K., Kimura T., Kihara T., Tachibana M., Tokunaga M. Capacitive detection of magnetostriction, dielectric constant, and magneto-caloric effects in pulsed magnetic fields. *Rev. Sci. Instrum*. 2020;91:105103. https://doi.org/10.1063/5.0010753
12. Tam A.C., Schroeder H. A new high-precision optical technique to measure magnetostriction of a thin magnetic film deposited on a substrate. *IEEE Trans. Magnetic*. 1989;25(3):2629–2638. https://doi.org/10.1109/20.24502
13. Samata H., Nagata Y., Uchida T., Abe S. New optical technique for bulk magnetostriction measurement. *J. Magn. Magn. Mater*. 2000;212(3):355–360. https://doi.org/10.1016/S0304-8853(99)00832-X
14. Hrabovska K., Zivotsky O., Rojicek J., Fusek M., Mares V., Jirakova Y. Surface magnetostriction of FeCoB amorphous ribbons analyzed using magneto-optical Kerr microscopy. *Materials*. 2020;13(2):257. https://doi.org/10.3390/ma13020257
15. Poore M., Kesterson K. Measuring the thermal expansion of solids with strain gauges. *J. Test. Eval*. 1978;6(2):98–102. https://doi.org/10.1520/JTE10926J
16. Khan M.A., Dumstorff G., Winkilmann C., Lang W. Investigation on noise level in AC- and DC-bridge circuits for sensor measurement systems. In: *18th GMA / ITG Conf. Sensors and Meas. Systems*. 2016. P. 601–605. http://doi.org/10.5162/sensoren2016/P4.4
17. Chashin D.V., Burdin D.A., Fetisov L.Y., Economov N.A., Fetisov Y.K. Precise measurement of magnetostriction of ferromagnetic plates. *J. Sib. Fed. Univ. Math. Phys*. 2018;11(1):30–34. https://doi.org/10.17516/1997-1397-2018-11-1-30-34
18. Nyquist H. Thermal Agitation of Electric Charge in Conductors. *Phys. Rev.* 1928;32:110–113. https://doi.org/10.1103/PhysRev.32.110
19. Hooge F.N. 1/f noise is no surface effect. *Phys. Lett. A.* 1969;29(3):139–140. https://doi.org/10.1016/0375-9601(69)90076-0
20. Voss R.F., Clarke J. Flicker (1/f) noise: equilibrium temperature and resistance fluctuations. *Phys. Rev. B*. 1976;13(2):556–573. https://doi.org/10.1103/PhysRevB.13.556
21. Walter D., Bulau A., Zimmermann A. Review on excess noise measurements of resistors. *Sensors*. 2023;23(3):1107. https://doi.org/10.3390/s23031107

About the Author

Dmitry A. Burdin, Cand. Sci. (Phys.-Math.), Senior Researcher, Scientific and Educational Center "Magnetoelectric Materials and Devices," MIREA – Russian Technological University (78, Vernadskogo pr., Moscow, 119454 Russia). E-mail: phantastic@mail.ru. ResearcherID N-9597-2016, RSCI SPIN-code 8152-3011, https://orcid.org/0000-0002-2648-0511

Об авторе

Бурдин Дмитрий Алексеевич, к.ф.-м.н., старший научный сотрудник, НОЦ «Магнитоэлектрические материалы и устройства», ФГБОУ ВО «МИРЭА – Российский технологический университет» (119454, Россия, Москва, пр-т Вернадского, д. 78). E-mail: phantastic@mail.ru. ResearcherID N-9597-2016, SPIN-код РИНЦ 8152-3011, https://orcid.org/0000-0002-2648-0511

Translated from Russian into English by K. Nazarov
Edited for English language and spelling by Thomas A. Beavitt